Perturbative Studies of Transport Phenomena in Fusion Devices

F. Ryter, R. Dux, P. Mantica[1], T. Tala[2]

Max-Planck-Institut für Plasmaphysik, EURATOM/MPI Association,
Boltzmannstrasse 2, D-85748 Garching, Germany

[1] Istituto di Fisica del Plasma, EURATOM/ENEA-CNR Association, 20125 Milano, Italy

[2] Association EURATOM-Tekes, VIT, PO Box 1000, FIN-02044 VTT, Finland

Abstract. Perturbative experiments are essential to understand the complex transport phenomena in fusion plasmas. The perturbative methods used for transport studies are summarised and the main properties discussed. Based on this approach, transport of particles, heat and momentum has been intensively investigated. The main results obtained for the different channels are described and illustrated with selected examples.

1. Introduction

Understanding transport of the different channels, heat, particles and impurities, toroidal momentum, is essential to predict and optimise future fusion reactors based on magnetic confinement. Significant progress on transport physics has been achieved in the last decade thanks to developments in both theory and experimental possibilities. Experimentally, transport can be investigated at equilibrium under steady-state conditions through the balance equation of the considered quantity. In addition, it is well-known in physics and engineering that the response of a system to a small perturbation around equilibrium yields further information. This method, also proven very fruitful to study transport in fusion plasmas, is known as "perturbative transport" or "transient transport" approach. Combining steady-state and perturbative analyses yields the most complete information to understand transport physics in terms of macroscopic quantities. In the present work the perturbative approach is introduced and recent important results are described. This is not an exhaustive review, but the bibliography provides a sufficient basis for the interested reader to find more information in the literature.

Transport in fusion devices is caused by collisions, so-called "neoclassical transport", and by micro-turbulence, "turbulent transport", see e.g. overviews [1, 2]. The relative weight of these two contributions to overall transport depends on the device, plasma conditions and transport channel, [2]. Electron heat transport is strongly dominated by turbulent transport in tokamaks and at least in large stellarators. For ion heat transport, both turbulent and neoclassical transport contribute. Electron particle transport is dominated by turbulence, whereas for ions and impurities both contributions must be considered. Toroidal angular momentum transport is driven by turbulence.

Turbulent transport in the core of present fusion devices, in particular tokamaks, is mainly caused, in the ion branch by the Ion Temperature Gradient instability (ITG), in the electron branch by the Trapped Electron Modes (TEM). The wave length of these modes is of the order of the ion Larmor radius. The Electron Temperature Gradient

modes (ETG), with much shorter wave length, may also contribute to electron heat transport in same cases. These modes have in common to be unstable above a threshold in normalised temperature gradient, $-R\nabla T/T = R/L_T$, where R is the major radius. For the TEM and ETG instabilities, the threshold is on the electron temperature and for the ITG on the ion temperature, whereas the density gradient, R/L_n, also contributes to destabilising the TEM, [2]. Transport driven by an instability is zero below the corresponding threshold and increases above it with increasing gradient. The rate of increase above the threshold is called "stiffness" in the present work.

The present work is structured as follows. The basis of perturbative transport is described in the next section. Perturbative experiments and results for different transport channels are described in the later sections following the order, particles, heat and momentum.

2. Basics of perturbative transport

In this section we briefly summarise the basic principles of perturbative transport, the reader being referred to the reviews [3, 4] for details.

Transport of a quantity y is governed by its continuity equation

$$\frac{\partial y}{\partial t} = -\nabla \Gamma_y + S_y \tag{1}$$

where Γ_y is the flux and S_y are sources and sinks. This equation is the basis of the standard diffusion equation. The physics of transport phenomena is contained in Γ_y. In plasmas, the various fluxes are related to corresponding gradients by the transport matrix, in which the diagonal terms represent the respective diffusion coefficients and the off-diagonal ones the coupling between transport channels, see e.g. [3]. Transport is determined locally by the relevant quantities. The flux for quantity y can be written in a general way as:

$$\Gamma_y = -D_y \nabla y + V_y y \tag{2}$$

where D_y and V_y are respectively diffusion and convection coefficients. The off-diagonal terms can be all cast in V_y, as explained for example for density in [5]. In steady state, D_y and V_y cannot be separated and the flux is written with an effective diffusivity, $\Gamma_y = -\chi_y^{eff} \nabla y$. In the core of fusion plasmas, the quantities considered here are very quickly equilibrated on the magnetic surfaces, reducing transport to its radial component. Only their radial profiles are considered and ∇ in the above equations is taken along the radius. Whereas R and r are major and minor radius of the toroidal plasma, ρ is a normalised radius related to the magnetic surfaces, varying from zero in the plasma centre to unity at the edge. For peaked profiles of y, which is the most general situation, ∇y is negative.

The physics of transport for quantity y is contained in D_y and V_y which generally depend on plasma parameters, in particular temperatures, density, and their gradients. These dependences are of crucial importance in transient experiments because the perturbation can, through them, induce variations of D_y and V_y which will then be reflected in $\nabla\Gamma_y$ in Eq. 1. This is evidenced when the above equations are linearised to investigate the behaviour of the perturbation, see [3, 4]. This important property was first recognised in [6] for electron heat transport, generalised and discussed in detail in [7]. The most important consequence is that D_y deduced from steady-state and perturbative analyses differ significantly if D_y depends on plasma parameters which are also perturbed, for instance ∇y or y.

In transient transport experiments, a perturbation of Γ_y is induced with an adequate actuator to which the system responds with variations of y and ∇y according to Eqs. 1 and 2. This yields in particular the relation between flux and gradient according to Eq. 2, around the equilibrium point. Depending on the channel to be investigated and on the physics aim of the experiment, the method of analysis may vary, but the basic principles remain the same.

The above equations provide the general frame of the transport analyses. Adopting the usual notations, they are written for the various channels as follows:

- Particle transport, with $(j = e)$ for electrons and $(j = Z)$ for impurities:

$$\frac{\partial n_j}{\partial t} = -\nabla \Gamma_j + S_j \qquad \Gamma_j = -D_j \nabla n_j + V_j n_j \tag{3}$$

  where n_j is the particle density;

- Heat transport, with $(j = e)$ for electrons and $(j = i)$ for ions :

$$\frac{3}{2}\frac{\partial (n_j T_j)}{\partial t} = -\nabla (q_j + \frac{5}{2}\Gamma_j T_j) + S_j \qquad q_j = -n_j \chi_j \nabla T_j + n_j V_j T_j \tag{4}$$

  where q_j and T_j are respectively heat flux and temperature;

- Toroidal angular momentum, dominated by the ions:

$$R m_i \frac{\partial (n_i v_{tor})}{\partial t} = -\nabla \Gamma_\phi + S_\phi \qquad \Gamma_\phi = -R m_i n_i (\chi_\phi \nabla v_{tor} - V_\phi v_{tor}) + \Gamma_{RS} \tag{5}$$

  with m_i ion mass, v_{tor} toroidal velocity, S_ϕ represents the different torque components and Γ_{RS} is the flux induced by the "residual stress" (Sect. 5).

Finally, it should be noted that D_y and V_y for one channel may depend on quantities of another channel, for instance V_e depends on T_e, [5], leading to coupling between channels and equations.

The perturbation may be excited externally by the required actuator, or internally by a plasma change, a typical example being the internal magneto-hydrodynamic "sawtooth instability", first discovered in 1974 [8], reviewed in [9]. The choice of the excitation, which may be a single pulse, a cyclic perturbation (modulation), or a step, depends on the experimental possibilities and on the goal of the study. Ideally, the excitation should be small enough to minimise perturbation of quantities others than that to be studied, and short pulses or modulation are better suited than steps. Single short pulses are widely used for impurity transport, whereas modulation is preferred for the other channels. In the case of modulation, the relevant perturbation can be advantageously extracted from the experimental data with correlation methods, e.g. Fourier transform (FFT). This improves the signal-to-noise ratio and allows to minimise the magnitude of the perturbation. The FFT results exhibit general properties which are worth summarising here. As an external modulated perturbation is generally applied

with a well defined frequency f_{mod} (pulsation ω_{mod}), the FFT exhibits a frequency spectrum with narrow peaks exactly at f_{mod} and possibly higher harmonics, depending on the modulation scheme. At each radial position of the measurement, one gets FFT amplitude and phase at f_{mod} and harmonics. The ensemble of measurement points provides radial profiles of amplitude and phase whose shape is determined by the sources and by the propagation of the perturbation. For pure diffusive propagation in a region free of modulated source, the amplitude profile decreases exponentially with a decay length, $\lambda = \sqrt{2D_y/\omega_{mod}}$, which must lie in an adequate range to ensure good experimental conditions. It should be large enough to allow measurable amplitude in the region of interest, but remain smaller than the typical plasma size to avoid the influence of the plasma boundary which might prevent interpreting the transport results locally. Under given plasma conditions, these requirements determine the best range for f_{mod}. The shape of the amplitude profile is affected by convection, whereas that of the phase is almost insensitive to convection. The effect of convection on amplitude decreases with increasing f_{mod}, [10], and a scan in f_{mod} is useful to sort out diffusion and convection. If the analysis is not carried out in a region free of modulation source, this must be taken into account, which generally requires modelling to interpret the experiment.

3. Particle and impurity transport

In fusion plasmas the peripheral particle source plays the major role. Sometimes, additional particle sources in the core due to Neutral Beam Injection or pellet injection also contribute. As recognised three decades ago, the peaked electron density profiles generally observed in fusion devices cannot be explained by pure diffusion and implies the existence of an inward convection, "particle pinch" [11]. The physics origin of the pinch can be due to the neoclassical Ware pinch in tokamaks only, and to turbulent transport through thermodiffusion and curvature pinch, see review [5] and references therein. For impurities also, both diffusion and convection are required to explain the observed transport behaviour, induced by neoclassical and turbulent transport.

As the particle sink is *exclusively* located at the plasma edge, in the absence of core particle source, the particle flux in steady-state is rigourously zero, reducing the flux equation to $\nabla n_j/n_j = V_j/D_j$. Experimentally this yields only V_j/D_j and perturbative studies are required to explore the dependence of Γ_j versus $\nabla n_j/n_j$ and separate D_j and V_j.

Among the main plasma species, only electrons can be studied in perturbative experiments because the concentration of the main ions, hydrogen and deuterium, cannot be measured directly. In contrast, the transport properties of a large variety of impurities have been studied in dynamical investigations.

3.1. Electron particle transport

Pioneering experiments on the response of electron density to step-wise gas puffing [12, 13] or gas modulation [14] evidenced the particle pinch. The basis of electron particle transport studies with gas puff modulation, described in detail in [15], is still used nowadays. Since this initial work, a moderate activity on this field has developed, in both stellarators [16, 17, 18] and tokamaks [19, 20, 21, 22, 23, 24, 25], for older results see [3, 4].

The usual method consists in modulating n_e with an adequate time-dependent gas injection. As in the initial studies, the measurement of the electron density response is, still in most of the cases, obtained from interferometry. The measurement is line-integrated and directly affected by the modulated electron source in the edge region, [15], which must be taken into account in the analysis. The usual scheme of the analysis consists in modelling the modulation of the interferometer lines of sight by solving the time-dependent transport equations. The FFT amplitude and phase yielded for the simulated lines of sight are matched to the experimental ones by adjusting the D_e and V_e profiles.

All the published results yield a strong pinch in the outer part of the plasma. Depending on plasma type and device, the particle pinch is found significant in the region extending

from the very edge up to about $\rho = 0.7 - 0.4$. The strength of the pinch compared to that of diffusion, $-RV_e/D_e$, reaches 2 to 5 in the experiments. This is why the particle pinch can be clearly detected experimentally, whereas its effect would be buried in the experimental uncertainties for pinch strength below ≈ 1.5, [15]. A good choice of the modulation frequency is important: too high would yield low modulation signals and also wipe out the pinch effect, but if it is too low, the characteristics of the radial propagation cannot be resolved.

It should be underlined that, D_e depending in particular strongly on ∇n_e [5], the value deduced from perturbative experiments is expected to be higher than that required to reproduce the density profiles in steady-state, even taking V_e into account. The comparison of the perturbative D_e profile with that required to reproduce the steady state profiles is available in some cases. Within the uncertainties, the steady-state density profiles could be reproduced satisfactorily using the perturbative coefficients in the TEXT tokamak [15]. In the ASDEX Upgrade [20] and DIII-D [22] tokamaks, D_e/V_e required for a good match with the equilibrium profile should be about 50% lower, in agreement with the assumption that D_e depends on at least ∇n_e. Other effects, such as n_e or T_e modulation could also play a role. Indeed, a correlated T_e perturbation is observed in gas modulation, [26], but only rarely analysed.

As discussed in [5], the particle pinch required to explain the peaking of density profile is clearly attributed to off-diagonal terms. The pinch revealed by perturbative experiments is most probably due to the same terms, but this remains to be explicitly demonstrated. It seems that, taking the advantage of existing local density measurements, new perturbative studies of electron particle transport should be envisaged, as well as comparison with theory which progressed in the recent years.

3.2. Impurities

The term "impurity" includes all ions which are not the main plasma ions, H^+ or D^+ in present devices. Helium is an impurity, except in the case of helium plasmas. Tritium

will not be an impurity in fusion reactor, but its transport has been studied at trace level, as an impurity, in JET and TFTR.

In the case of impurities, both neoclassical and turbulent transport play a role and the goal of the studies is to assess their respective contributions. As the transport properties depend on Z, comparing different impurities in the same plasmas provides the most complete information.

In experiments on impurity transport, the perturbation consists in injecting a small amount of the species to be investigated. Gas pulses, laser ablation or pellets for non-gaseous impurities, are used. To keep the level of impurity as low as possible and avoid other spurious effects, modulation is in general not used, although possible with gaseous impurities, [27, 23]. The choice of the impurity depends on the goal of the experiment and should be matched to the plasma parameters.

The situation for impurities differs fundamentally from that of electrons for three reasons. Firstly, before the injection of an impurity its concentration n_Z is generally zero. Secondly, the injected amount can generally be kept low enough such that the other equilibrium plasma parameters are not affected, "trace level". Thirdly, as D_Z and V_Z do not depend on n_Z or ∇n_Z, at least at trace level, they can be considered constant for the given plasma and therefore correspond to the steady-state values.

The impurity injection, generally short, creates a radially very localised source at the edge, therefore a very strong *positive* radial gradient in n_Z at the plasma periphery. This steep gradient quickly flattens through diffusion while the injected impurity propagates towards the plasma centre. The time evolution slows down, n_Z reaches a maximum which depends on radius to gradually decrease afterwards. The decreasing phase is fundamentally different for impurities which recycle at the edge and for those which do not. For non-recycling impurity the sink can be assumed to be 100% and the time evolution during the decay time contributes to the analysis of D_Z and V_Z. In contrast, for recycling impurities, the decay is strongly determined by pumping. If the sink is not strong enough, the time evolution of n_Z does not allow to separate V_Z and D_Z

because the system is too close to equilibrium. The diagnostics used to monitor the injected impurity must be fast enough to follow with accuracy the time evolution and offer radial resolution.

Examples of time evolutions for a non-recycling element, silicon, and a recycling one, helium, are illustrated in Fig. 1, from the ASDEX Upgrade and DIII-D tokamaks. The choice of this comparison is justified by the fact that the two devices are of the same size and the H-mode plasmas considered have comparable parameters. Furthermore, it is known from other studies that, for both ASDEX Upgrade, [28], and DIII-D, [29], ITG turbulence plays a dominant role in such discharges.

In both cases, the increase of the time traces after the injection is clearly slower in the center compared to the edge, reflecting the inwards propagation governed by transport. After the maximum has been reached, the Si traces decay rapidly whereas those for helium remain almost constant due to recycling. Note the values of n_{Si} which reach at most $10^{17}m^{-3}$, corresponding to a maximum silicon concentration of about 0.3% at the edge and less in the center.

The transport analysis requires n_Z, which can be measured locally in rare cases, otherwise line-integrated. One generally reconstructs the measurements with an impurity transport code by adjusting the n_Z profile through V_Z and D_Z, see e.g. [32, 30, 33]. The result from this method are shown by the dashed red lines in Fig. 1 left column. In cases where n_Z is available locally, the "flux-gradient method", only based on the data, initially applied to electron transport with pellets [34], can be used. At a given position, $\Gamma_Z(t)$ and $\nabla n_Z(t)$ deduced from the measurement allow to plot Γ_Z/n_Z versus $\nabla n_Z/n_Z$. Following Eq. 3, this yields a linear dependence with offset V_Z and slope $-D_Z$. The result of this method is shown in Fig. 1.c for $\rho = 0.3$. In this approach, the experimental uncertainties of the measurement provide a direct estimate of the error bars on V_Z and D_Z. Based on this approach, numerous results have been obtained, some of them are presented below.

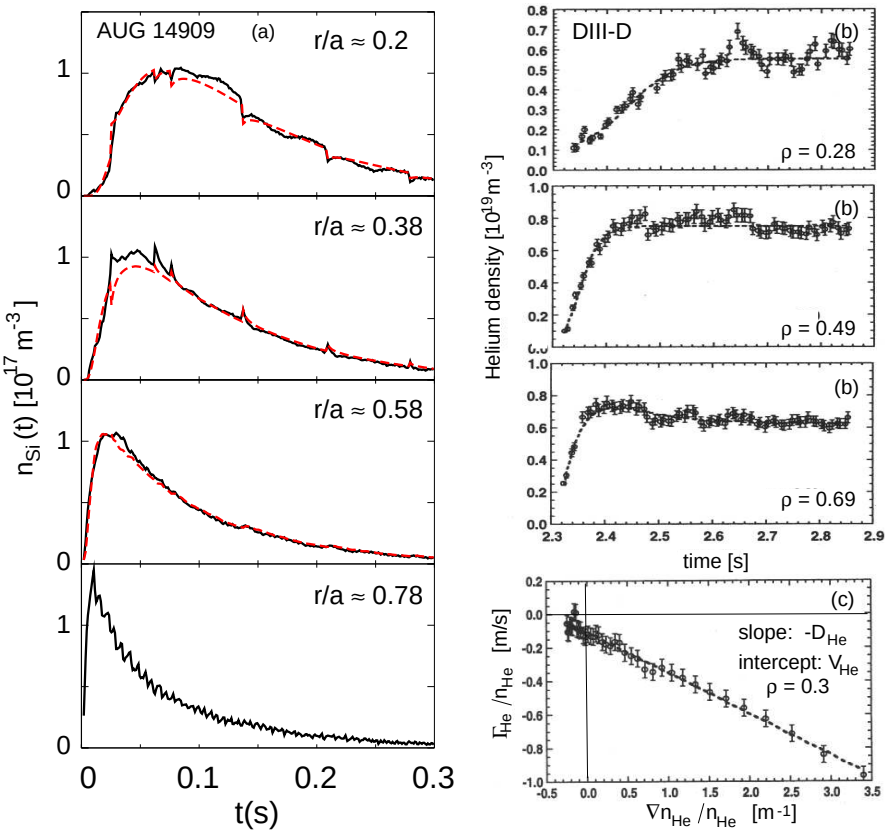

Figure 1. *Left panel: Time traces following silicon laser ablation measured with a soft X-ray diagnostic (black solid lines) at different radii in ASDEX Upgrade. The effect of a few sawteeth is visible. The red dashed lines are from modelling. After [30], copyright IOP.*

Right panel, plots (b): Time traces produced by a helium puff, measured with charge exchange recombination spectroscopy in DIII-D. The lines are fits to the data used for the analysis. Plot (c): Flux-gradient diagram of the same experiment at $\rho = 0.3$. *After [31],copyright AIP.*

Tritium

It is worth underlying that transport of tritium has been investigated in the "trace tritium experiments" carried out in JET and TFTR, using short tritium puffs. The evolution of n_T has been monitored through the 14.3 MeV fusion neutrons [35, 36, 37, 38]. The measurement is indirect and the analysis requires modelling to link the measured neutron fluxes with n_T. The results, so far the only transport measurements of a

hydrogenic ion, have indicated a strong contribution from turbulent transport with pinch in the outer half of the plasma, whereas convection is close to zero further in and transport close to neoclassical. The diffusion is comparable to the ion heat diffusivity.

Helium

In a reactor, α-particles produced by the fusion reactions will provide the heating power but also the "helium ash", an unavoidable impurity which will dilute the D-T fuel and reduces the fusion efficiency. Its concentration is expected to reach several percents and it is essential to know the transport properties to reduce it as much as possible. In perturbative experiments, n_{He} following a gas puff is measured locally with charge exchange spectroscopy, [39, 40, 41, 31, 42, 23]. The flux-gradient method is generally used, sometimes compared with impurity transport simulations, [40, 42].
The results reported in the above references are comparable to those for tritium. The pinch is high at the plasma edge and decreases strongly towards the centre, Fig. 2 right panels. The ratio $-RV_{He}/D_{He}$ is around 3 at mid-radius and further out. The values for D_{He}, which strongly decrease from the edge to the centre, are close to χ_i. Worth noting is the transport analysis of the helium ash produced by the fusion reactions in the D-T experiments in TFTR, [41].

Other impurities

Apart from tritium and helium, a large choice of impurities covering a wide range in Z is available. They are monitored with spectroscopic measurements, very limited by the small number of lines of sight, and almost always with soft X-ray cameras with a large number of lines of sight, line-integrated but with good time resolution. Numerous studies have been performed in several devices and different plasma types, [32, 43, 44, 45, 46, 33, 47, 48]. The analysis of transport physics and comparison with neoclassical and turbulence-driven theory yield a wide range of results which vary with plasma type, heating deposition profile and Z of the considered impurity. The results

indicate that both neoclassical and turbulent transport play a role with varying weight.

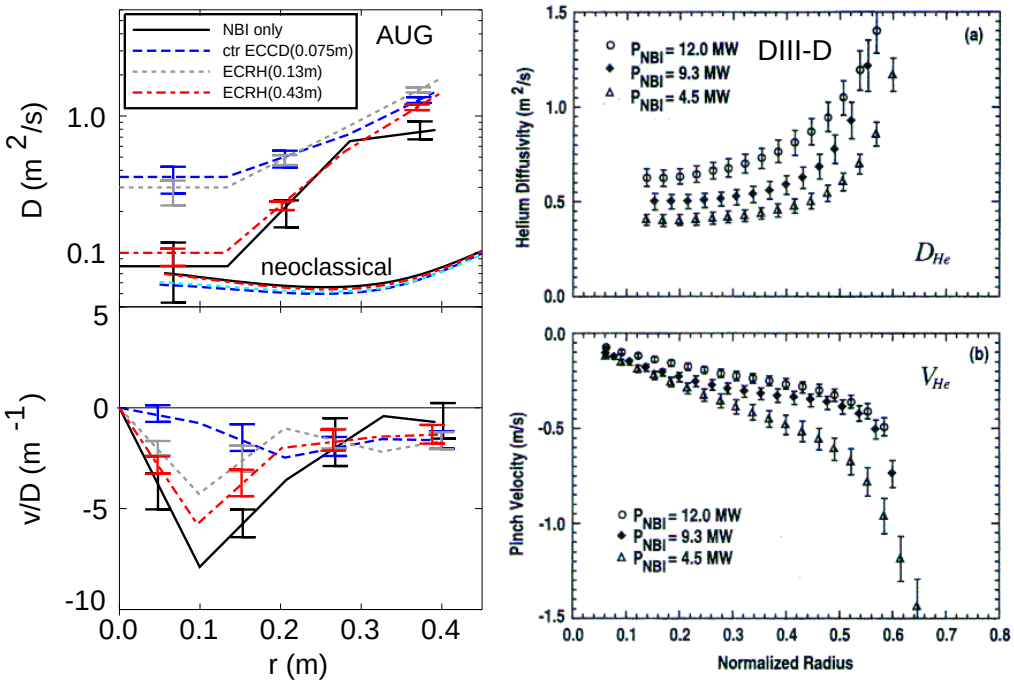

Figure 2. *Left panel: D and V/D for silicon from the experiment shown in Fig. 1. The blue curves (ctr-ECCD 0.075m) correspond to a case with high central heating. After [30], copyright IOP. Right panel: D and V for helium in DIII-D corresponding to data shown in Fig. 1. After [31], copyright AIP.*

Two examples, corresponding to the silicon and helium experiments of Fig. 1 are illustrated in Fig. 2. They reflect the general results: increase of D and decrease of V with heating power. The contribution of turbulent transport is strong in the outer half of the plasma, whereas neoclassical transport often dominates in the central plasma, roughly $\rho < 0.3$, except when localised heating is deposited there. Summarising all the results is out of the scope of the present paper and the reader is referred to [49] for an overview and in particular for the dependence on Z.

4. Heat transport

Heat transport is driven in the electron and ion channels. Amongst the two, electron heat transport is the most studied by perturbative experiments, for which adequate

actuators and measurements have been available for a long time. In contrast, results on perturbative ion heat transport are rare, mainly because of the limited experimental possibilities. Therefore this section is focused on the electron channel, the few results on ions being summarised at the end.

The first application of the perturbative method to investigate electron heat transport dates back to 1974 with a pulse of electron heating in the FM-1 Spherator, [50]. Three years later, the electron heat diffusivity deduced from the propagation of heat pulses induced by sawtooth crashes has been reported to be much faster than assuming χ_e from power balance, [51]. Following these first attempts, numerous experiments and analyses yielded the same conclusion. The results until 1995 were reviewed in [3, 4]. Demonstrated in 1987, [6], the importance of the dependence of χ_e upon ∇T_e was an essential step in understanding perturbative experiments. Calling respectively $\chi_e^{PB} = -q_e/(n_e \nabla T_e)$ and χ_e^{HP} the heat diffusivities deduced from power balance and propagation of the perturbation, it has been shown that

$$\chi_e^{HP} = \chi_e^{PB} + \frac{\partial \chi_e}{\partial(\nabla T_e)} \nabla T_{e,0} \tag{6}$$

$T_{e,0}$ being the equilibrium temperature, assuming that χ_e depends on ∇T_e only and neglecting convection. This explains the generally observed result $\chi_e^{HP} > \chi_e^{PB}$. Following Ref. [3, 4], examples of possible q_e dependences on ∇T_e are illustrated in Fig. 3.

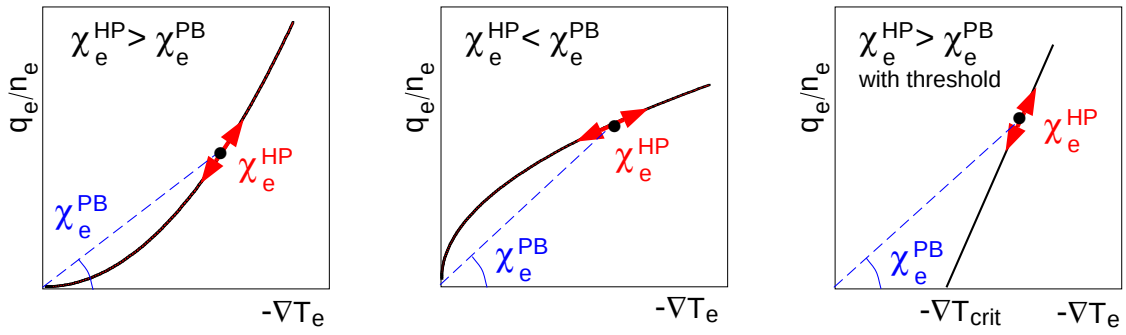

Figure 3. *Possible cases for q_e versus ∇T_e.*

Assuming slab geometry, an estimator of χ_e^{HP} can be inferred directly from the FFT profiles of the experimental data, originally developed in [52], see [3, 10, 4] for a comprehensive description. From the profiles of amplitude (A) and phase (φ) provided by the FFT, three expressions can be derived:

$$\chi_{exp}^{amp} = \frac{3\omega_{mod}}{4(A'/A)^2} \qquad \chi_{exp}^{phi} = \frac{3\omega_{mod}}{4\varphi'^2} \qquad \chi_{exp}^{HP} = \sqrt{\chi_{exp}^{amp}\chi_{exp}^{phi}} \tag{7}$$

where A' and φ' mean radial derivatives. In general, $\chi_{exp}^{phi} \geq \chi_{exp}^{amp}$ due to damping effects, but for high f_{mod}, their values converge towards χ_{exp}^{HP}, in which the damping terms cancel exactly. This is a widely used estimator. Corrections for cylindrical geometry and density gradient can be included, [10].

As χ_e^{PB} and χ_e^{HP} can be both determined experimentally, $\partial\chi_e/\partial(\nabla T_e)$ at the equilibrium point around which the perturbation is excited can be deduced. This is a precious information for physics understanding and a stringent constraint for comparison with theory.

Actuators

The main types of actuators used to excite the perturbation for electron heat transport are: electron heating, "cold pulse" induced by impurity injection, naturally occurring sawtooth crashes in tokamaks only. Sawtooth crashes have been widely used in the past, but it should be underlined that they are often not a small perturbation and "ballistic effects", for instance, can affect the transport interpretation [53, 54]. Indeed, χ_e^{HP} deduced from sawtooth pulse propagation can yield significantly larger values than those yielded by more controlled ECRH modulation [55].

Impurity injection cools transiently the plasma periphery and the inward propagation of this "cold pulse" can be followed in the T_e measurement. This method has, for heat transport studies, the drawback that the edge perturbation is abrupt and creates at the edge a strong negative gradient which might induce a different or additional propagation mechanism.

An ideal actuator for electron heat transport studies is power modulation of Electron

Cyclotron Resonance Heating. The plasma is heated by micro-wave beams in the electron cyclotron frequency range, [56, 57]. Very localised power deposition, with 100% absorption by the electrons and flexible radial position can be achieved. The size and frequency of the modulation can be matched to the needs. The combination of ECRH with the measurement of T_e with high time and radial resolutions, provided by the Electron Cyclotron Emission diagnostic, offers the best conditions for perturbative experiments dedicated to electron heat transport. These possibilities were further developed since review [4], yielding new results. Some of the main contributions to physics understanding are described in the following.

Physics of TEM-driven transport

Several experiments on perturbative electron heat transport have been performed with dominant electron heating and therefore in the TEM-driven transport regime for which transport increases above a threshold. In such cases, the ITG contribution to heat transport is small. An important milestone in 2001, was the ability of a simple model based on the existence of a threshold to reproduce simultaneously power balance and perturbative data from experiments under various ECRH conditions carried out in the ASDEX Upgrade tokamak [58]. It is generally called "critical gradient model" and was then successfully applied to other experiments in ASDEX Upgrade, [59, 60], DIII-D [61], JET [62], FT-U [63] and in comparisons between devices [64, 65]. As pointed out in [58], the model implies not only $\chi_e^{HP} > \chi_e^{PB}$ above the threshold, but also that χ_e^{HP} exhibits a step-like behaviour at the threshold, jumping from a low value ($\chi_e^{HP} = \chi_e^{PB}$) below the threshold, to the higher value just above it. Thus, in a scan of R/L_{T_e}, a jump of the experimental χ_e^{HP} would be an evidence for the existence of a threshold. This has been demonstrated in [60], illustrated in Fig. 4 a and b. The left panel shows q_e versus R/L_{T_e} which indeed exhibits a clear increase for $R/L_{T_e} > 2.8$, in agreement with TEM destabilisation as predicted by linear gyro-kinetic calculations. Correspondingly, plot 4.b shows a jump-like change at the threshold, strong for χ_e^{amp} and weaker for for

χ_e^{phi}, for reasons explained in Ref. [60]. The data are well reproduced with the critical gradient model, open symbols in the two plots.

Another main property of the TEM instability predicted by theory is its stabilisation at high collisionality. By increasing collisionality in ASDEX Upgrade, ECRH modulation experiments exhibited a strong decrease of χ_e^{HP}/χ_e^{PB} which eventually clearly drop below unity, [60]. Stability calculations of turbulence indicated that plasma transport was changing from TEM to ITG dominated as collisionality increased. Therefore, at high collisionality, where the TEM was stable, the electron heat flux was driven by the ITG which, being driven by ∇T_i, has a very weak dependence on ∇T_e. This is illustrated in Fig. 4 c, a flux-gradient diagram where the slope deduced from χ_e^{HP} is indicated for points at different collisionalities, exhibiting $\chi_e^{HP} > \chi_e^{PB}$ at low collisionality and $\chi_e^{HP} < \chi_e^{PB}$ at high collisionality. The electron heat flux yielded by the gyro-kinetic calculations for the TEM and ITG branches exhibit the same slope as that yielded by the perturbative analysis at low and high collisionality respectively.

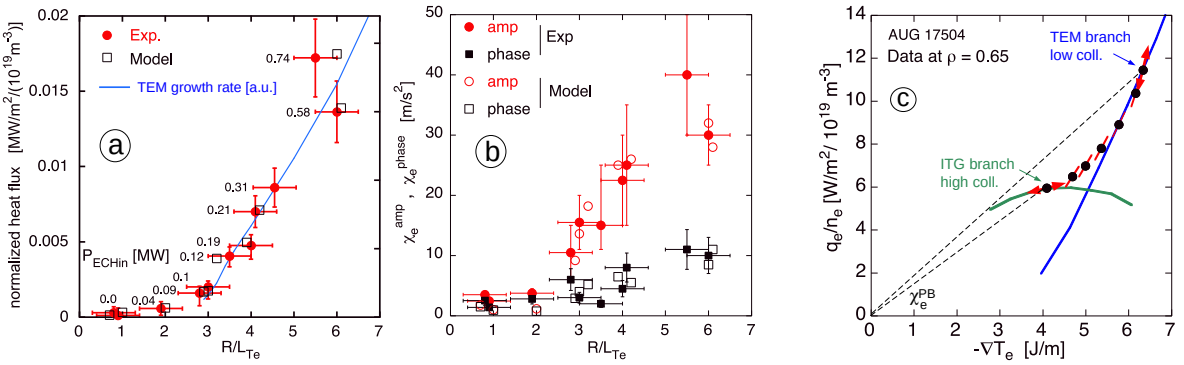

Figure 4. *Panels a and b: evidence for TEM threshold. a: Normalised heat flux versus R/L_{T_e}, b: χ_e^{amp} and χ_e^{phi} exhibiting the "jump" caused by $\partial q_e/\partial \nabla T_e$, [60]. Panel c: Effect of collisionality on transport. Heat flux versus gradient diagram, in a collisionality scan causing a transition from TEM to ITG. The red arrows indicate the slope $\partial q_e/\partial \nabla T_e$ deduced from the modulation data.*

Comparison tokamak-stellarator

As stellarators have no sawteeth, the comparison with tokamaks is focused on ECRH and cold pulses. The literature on perturbative heat transport in stellarators is less abundant than that for tokamaks. Two papers deal with comparisons of perturbative transport studies in stellarators and tokamaks [66, 67]. Whereas χ_e^{HP}/χ_e^{PB} in tokamaks is generally larger than 2, in stellarators this ratio is always lower than 2 and close to unity in most of the cases [68, 69, 66, 70, 71, 67]. This difference clearly indicates that the dependence of χ_e on ∇T_e in stellarators is weak, as explicitly pointed in the above references. Whereas a T_e dependence of χ_e has been discarded in the W7-AS stellarator, [68, 69, 66], a significant T_e dependence is found in LHD plasma investigated with cold pulses, [67]. Similarly to the tokamak situation, in LHD also, turbulence plays a major role in electron heat transport for which a threshold in R/L_{T_e} has also been found, [67]. The weak ∇T_e dependence in stellarators calls for dedicated experimental and theoretical comparisons of turbulence properties in the two kinds of devices.

Internal transport barriers

Under certain conditions, so-called Internal Transport Barriers can be created by a radially localised reduction of transport in the plasma core in both tokamaks [72] and stellarators [73]. Perturbative experiments were carried out under such conditions, in the JET and JT-60U tokamaks, as well as in the TJ-II and LHD stellarators. The propagation of cold pulses in JET [74], JT-60U [67] and LHD [75, 67], exhibit similarities, in particular a transport reduction in the ITB. A radially localised transport reduction in the ITB has clearly been evidenced using electron heating power modulation in JET with discussion of ITB physics [76, 77, 78], in LHD [75] and TJ-II [79]. Related to this topic, a dynamical transport analysis of electron ITBs, based on spontaneous transitions, is reported for the W7-AS stellarator, [80].

Ion heat transport

Perturbative experiments dealing with ion heat transport are very rare due to the lack of adequate ion heating in most of the devices. An analysis of the propagation of the ion heat pulses following sawtooth crashes was reported in [81]. Rather recently, experiments have been carried out in JET using ICRH ^{3}He minority scheme with which ions can be heated efficiently and locally [82]. Power modulation and measurement of the induced T_i perturbation allowed to analyse χ_i^{HP} and compare it with χ_i^{PB}, [83]. In particular, the expected convergence of χ_i^{amp} and χ_i^{phi} as function of f_{mod} was found, confirming the validity of the method for ions. The transport results yielded $\chi_i^{HP}/\chi_i^{PB} \approx 2$ and revealed, under such conditions, a moderate ion stiffness. Other JET results, aiming at measuring the ion stiffness over a wide range of plasma parameters exhibited large changes in ion stiffness attributed to plasma rotation [84]. Some of these points could, in addition, be supported by the ion modulation method developed in [83]. Clearly, further perturbative studies of ion heat transport would be desirable to extend the range of results and comparison with theory.

Heat convection

Whereas there is clear experimental evidence for particle pinch, the situation is unclear for heat pinch. Experiments have been carried out on electron heat pinch only, not on ion heat pinch. The observation of peaked temperature profiles despite off-axis heating are a common property in tokamaks. The existence of an electron heat pinch has been inferred from steady-state power balance in DIII-D plasmas exhibiting peaked T_e profiles despite off-axis electron heating [85, 86]. Convective effects were also reported in the RTP tokamak with ECRH heating [87], partly comparable to the DIII-D results. Heat pinch has been ruled out in the W7-AS stellarator [66].

Power modulation experiments are expected to provide convincing evidence of convection by a distortion of the amplitude profile, whereas phase is not affected. In RTP, ECRH modulation experiments exhibited a strong effect on amplitude in

agreement with a heat pinch [88, 89]. The analysis of ECRH modulation data in the flux-gradient diagram in DIII-D is not compatible with a heat pinch, at least in the outer part of the plasma, [90]. A flattening of the amplitude profile observed in the DIII-D modulation experiments reported in Ref. [61] is attributed to a heat pinch effect, [91]. Similar experiments carried out in ASDEX Upgrade [59, 60] also exhibited a flattening of the amplitude profile, which, however, is well reproduced with the critical gradient model, [60]. In ASDEX Upgrade, an extensive series of experiments was dedicated to the search of a heat pinch with off-axis ECRH, using power modulation [92]. The T_e profiles remained indeed peaked. In modelling with the critical gradient model a heat pinch was not required to sustain the peaked profiles in the central part, $\rho < 0.3$. Indeed, the residual ohmic heating power seems sufficient to sustain T_e just above the critical gradient as transport is very low there. However, in the region $0.3 < \rho < 0.6$, just inside of the ECRH deposition, the simulated profiles tend to be too flat or even hollow and a heat pinch (1 - 3 m/s) allows to reconcile simultaneously flat modulation amplitude profile and T_e shape in this radial region, [92]. Finally, as pointed out in [58], the temperature dependence of transport, as for instance exhibited by the critical gradient model, introduces an apparent convection term in perturbation experiments, making the search for an actual heat pinch caused by off-diagonal terms more difficult. A heat pinch is predicted by theory, caused by the thermodiffusion particle pinch and linked to density gradient: a strong heat pinch is expected under conditions for a strong thermodiffusion [93]. Simulations based on this effect reproduce the DIII-D steady-state results, [94, 95], while the effects of supra-thermal electrons is favoured in [96].

As experimental results and interpretations are not decisive, further dedicated experiments, guided by theory, seem to be desirable.

5. Momentum transport

In tokamak plasmas, the profile of toroidal rotation, v_{tor}, plays an important role for transport and MHD stability. The rotation profile is determined by momentum sources,

sinks and transport, see review [97] and references therein. Toroidal rotation can be driven by an external torque, such as NBI, but "intrinsic rotation" is also measured in the absence of external torque. For the latter, turbulence is considered as a possible momentum source [97, 98]. As reviewed in [97], various momentum sources can be active simultaneously with comparable magnitudes and with opposite signs. Therefore, the analysis of momentum transport generally requires elaborated assessment of sources and sinks and is more complex than the channels discussed in the previous sections.

The equations for momentum transport given above, (Eq. 5), include a flux term, the "residual stress", which takes into account effects of plasma parameters, see e.g. [98, 97]. Depending on the experimental conditions this term can be neglected or not. The neoclassical contribution to momentum transport is much smaller than for ion heat transport because the trapped particles do not contribute to momentum transport. Therefore, the major contribution to momentum transport is attributed to ITG-driven transport in which both diffusion and convection are important. Theory of turbulent transport predicts χ_i and χ_ϕ to be comparable: the Prandtl number, $P_r = \chi_\phi/\chi_i$ is expected to be close to unity. The analysis of steady-state experiments yields χ_ϕ^{eff}/χ_i, found to be around unity, but with large variations towards low values by up to one order of magnitude, as shown in early studies, [99, 100, 101, 102], and more recently [103, 104, 105]. This suggests the existence of a "momentum pinch" leading to $\chi_\phi^{eff} < \chi_\phi$. Indeed, recent theoretical studies indicate that the pinch should not be neglected [106, 107, 108]. This motivated recent perturbative experiments on momentum transport.

The existence of the momentum pinch has been indeed evidenced by perturbative experiments in pioneering experimental work using NBI torque modulation in JT60-U, [109]. In JFT-2M transients were induced by commuting the direction of the NBI, with respect to plasma current, between co-NBI and counter-NBI, [110, 111]. After an interruption of about 10 years, an intense experimental activity on the identification of χ_ϕ and V_ϕ using perturbative experiments recently developed in several tokamaks

utilising different actuators for the perturbation. Those can be braking at the plasma edge and torque modulation by NBI. In addition it has been observed that applying ECRH can strongly affect rotation [112, 113, 114, 115], which could also be used for perturbative experiment to investigate momentum transport. However, as the origin of ECRH effect on rotation is not clear yet, we focus here on experiments using braking and NBI modulation.

Perturbative edge braking

In JT60-U, modulation of perpendicular co-NBI and ctr-NBI beams has been applied simultaneously . This does not modify the applied torque directly but modulates the drag at the edge through the high level of fast ion losses [116, 117]. Analysing the propagation of the induced perturbation on v_{tor} from the edge to the center reveals a pinch. Edge braking experiments have also been carried out in NSTX [118, 105] and DIII-D [119] using external magnetic field perturbations. In both cases, the time-dependent transport simulations also require a pinch for a good match with experimental data.

Modulation of core applied torque

The analysis of perturbative momentum transport by NBI modulation is complex because the applied torque has a broad radial profile and no region free of modulated source exists. Therefore, an accurate calculation of the torque is essential. In addition, the NBI-induced torque has two main components with different radial profiles and time constants [120]. The slower one arises from the collisional transfer of the fast NBI ions as they are slowed down. The faster $j \times B$ component is caused by charge separation of the electron and ion created when an injected NBI neutral is ionised, due to their different trajectories. Fast ion losses also contribute and must be correctly accounted for.

In recent experiments, torque perturbation induced by NBI modulation has been used

in JET, [121, 122, 123], and by NBI pulses in DIII-D [119]. A finite pinch, V_ϕ, is definitely required in the transport simulations to match the measured rotation response in both devices. The most recent and complete experiments with NBI torque modulation are reported for JET in [124]. Similarly to the approach used for heat transport studies, a square wave modulation, at $f_{mod} = 8.33$ Hz, was used with duty-cycle of 33%, also exciting the 2^{nd} harmonic. The data quality allows to also analyse this higher frequency. The experimental v_{tor} data are Fourier-analysed, yielding amplitude and phase profiles. The results are interpreted by momentum transport simulations, including the modulated sources, which yields a time-dependent rotation profile. Its Fourier amplitude and phase profiles are then compared to the experimental ones and the transport coefficients profiles χ_ϕ and V_ϕ adjusted to match them. This occurs in 2 steps, taking advantage that the phase is almost not affected by the pinch velocity.

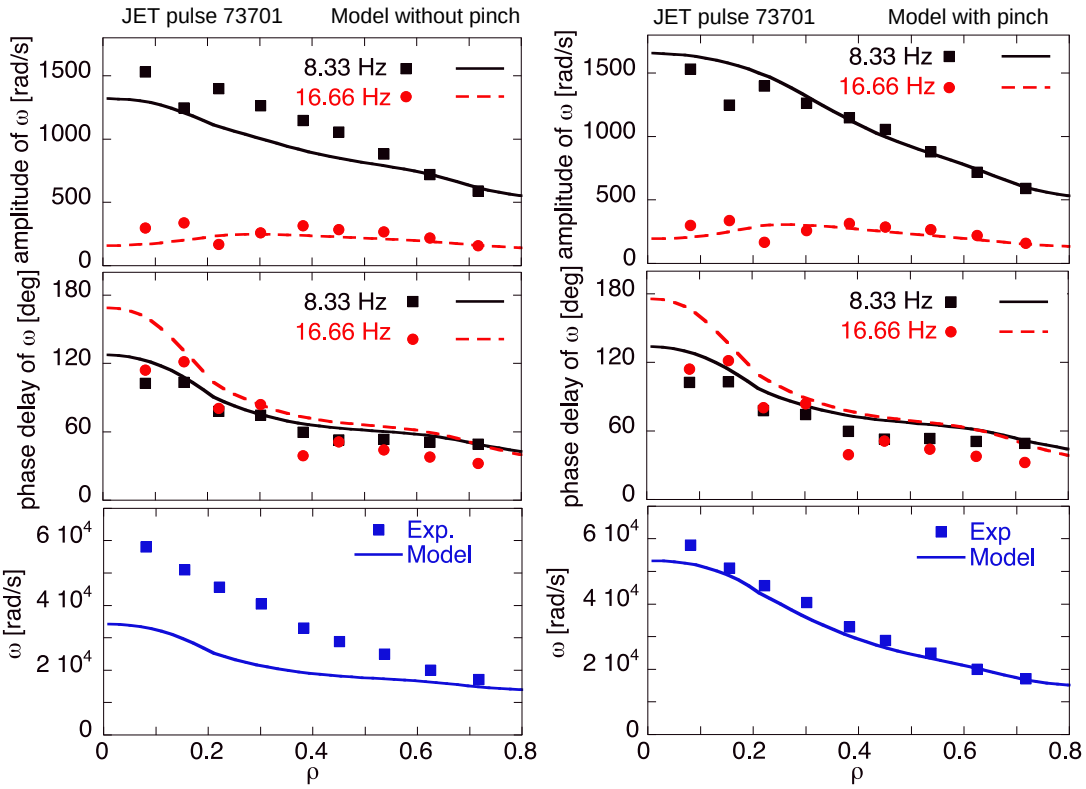

Figure 5. *Profiles of toroidal rotation, modulation amplitude and phase delay, points are for experimental data, line from modelling. After [124], copyright EURATOM.*

Firstly, the calculated phase is matched to the experimental data by adjusting χ_ϕ only. The FFT results are shown in Fig. 5, left plot. The calculated phase delays are in good agreement for the two frequencies, but amplitude at 8.33 Hz and time-averaged profiles are not matched at all, as expected if convection plays an important role. As second step, keeping χ_ϕ fixed, V_ϕ is adjusted until the simulation matches the experimental amplitude and time-averaged profiles of v_{tor}, the phase remaining unchanged. The result shown in Fig. 5, right plot, exhibits a good agreement for all three quantities at the two frequencies. It worth noting that, for the higher frequency, the effect of V_ϕ on the amplitude is small, as expected from the fact that the impact of convection on modulated data decreases with increasing frequency. It should also be underlined that the amplitude profile at the 2^{nd} harmonic exhibits a maximum at about mid-radius which is caused by the fact that the $j \times B$ contribution to the NBI torque dominates at higher frequency whereas the collisional part is smoothed out due to its long time constant. As for temperature modulation, here also an apparent pinch might contribute to the shape of the profile of the modulation amplitude, but the large difference between the modelling results with and without V_ϕ indicate that this is not a strong effect. This is due to the large contribution of V_ϕ to momentum transport. In these experiments P_r reaches up to 1.7 in the outer part of the plasma, [124].

Summarising, there is a broad basis of experimental evidence showing the existence of a momentum pinch. This effect is predicted by theory, [107, 108], and the experimental values agree well with these predictions [119, 105, 122, 123, 124], indicating that off-diagonal terms play a key role in V_ϕ. It should be pointed out that V_ϕ reaches values in the range 20 - 40 m/s at mid-radius such that the dimensionless ratio RV_ϕ/χ_ϕ lies in the range 3 to 5 in JET, [124], as well as in DIII-D and NSTX, [115]. Therefore, similarly to particle transport, the momentum pinch is large, allowing it to be clearly identified. It should be pointed out that experiments without external torque have also shown the existence of a momentum pinch, such as in Alcator C-Mod where the effect of an L-to-H transition on rotation profile has been analysed [125, 126]. This underlines

the universal character of the momentum pinch.

6. Coupling between channels and other results

In the above sections, studies of single transport channels were presented, but channels might be coupled. Perturbative experiments are efficient to reveal coupling through the response of a channel which is not that excited by the actuator. A typical example is the coupling between electron density and temperature, due in particular to thermodiffusion [5]. Astonishingly, very few perturbative experiments were dedicated to this topic, [127, 128, 80]. Another example is the coupling between electron and ion heat fluxes for the ITG-induced transport. This effect has been clearly indicated by the reaction of T_i to ECRH-induced T_e modulation in the DIII-D tokamak [129]. Further indication of this coupling is also suggested by the T_i modulation experiments in JET, [83]. A coupling between heat transport and current profile has also been revealed by spontaneous oscillations in Tore Supra [130]. It seems that the possibilities to investigate coupling by perturbative methods could be more extensively exploited than done so far.

In both tokamaks and stellarators, very fast reactions to perturbations, sometimes called "non-local transport" and appearing as discontinuities in the flux-gradient diagram, have been reported, in reaction to abrupt changes in heating power, [131, 132, 90], or cold pulses from impurity injection. In addition, an edge cold pulse may generate a temperature increase in the plasma centre, "polarity inversion". This topic, which seems to defy the causality principle, has been reviewed in [133] to which the reader is referred for more details. A complete discussion is out of the scope of this work, recent results were reported for stellarators, [134, 135, 136, 137, 138], and tokamaks, [139, 140, 141, 142], for JET [62] and reference therein. They certainly do not call the basis of transport into question, but indicate that elements might be missing under particular conditions. Possible interpretations have been discussed in [143, 144, 145, 146].

Perturbative experiments are used to address numerous other physics issues, some

examples are listed here. If the modulation frequency is high enough, the experimental amplitude and phase profiles reflect the deposition profile of the actuator, as applied to various heating methods, [147, 148, 149, 150, 151, 152, 70, 153]. Similarly, the power deposition can be deduced from the change of the time derivative of a quantity at the very beginning or end of a pulse, [154, 155, 156, 157], and references therein.

Modulation of electron heating has been used to study the heat flux pattern in the presence of an MHD mode [158, 159, 160].

Finally, in addition to sawtooth pulses, other spontaneous changes induce perturbations which can be used for transport understanding, [161, 162, 80, 163, 130, 164, 165].

7. Summary and Conclusion

The contribution of perturbative studies play a key role in understanding transport in fusion plasmas, as shown by the development over the last 2 decades. Such experiments allowed, for instance, to separate diffusion and convection, to assess the existence of turbulence threshold and to investigate coupling between transport channels. In comparisons with theory they reveal the importance of the off-diagonal terms of the transport matrix. The experiments require an adequate combination of actuators and measurements, which fulfil the requirement with different level of quality, depending on the channel to be investigated. Progress might be expected in this area. Good design of perturbative studies should be guided by theory to address the issues with an adequate choice of plasma parameters and vary the required quantities.

The studies on impurity and heat transport brought numerous results and these are still active fields of research. It seems that helium transport would gain from a revival. Momentum transport is very actively studied and further results can certainly be expected. The activity on electron particle perturbative transport is moderate and the recent vigourous activity on "density peaking" should be accompanied by transient transport experiments. Ion transport cannot be widely studied dynamically because of the lack of adequate actuators, but its understanding would greatly gain from more per-

turbative experiments. Finally, perturbative experiments are well suited to investigate coupling between channels and this subject would gain from more experiments.

As turbulence plays a major role in transport, measurements of fluctuations in perturbative experiments and comparison with turbulence calculations should be intensified. In the future, the analysis of perturbative experiments will probably require considering more than one channel. Perturbative experiments investigating different transport channels in discharges with comparable dimensionless plasmas parameters, or in scans of such variables, would be very valuable for physics understanding.

Acknowledgement

We warmly thank the many colleagues who kindly provided material on the work in their fields of activity: J.C. DeBoo, R. Guirlet, C. Hidalgo, G.M.D. Hogeweij, K. Ida, F. Imbeaux, A. Jacchia, T.C. Luce, W.M. Solomon, M. Yoshida, M.R. Wade. It is a great pleasure to acknowledge stimulating discussions with C. Angioni, for the present work and during the last years.

References

[1] W. Horton, Rev. Mod. Phys. **71** (1999) 735.

[2] X. Garbet et al., Plasma Physics and Controlled Fusion **46** (2004) B557.

[3] N. J. Lopes Cardozo et al., Plasma Phys. Controlled Fusion **32** (1990) 983.

[4] N. J. Lopes Cardozo, Plasma Phys. Controlled Fusion **37** (1995) 799.

[5] C. Angioni et al., Plasma Physics and Controlled Fusion **51** (2009) 124017 (14pp).

[6] B. J. D. Tubbing et al., Nucl. Fusion **27** (1987) 1843.

[7] K. W. Gentle, Phys. Fluids **31** (1988) 1105.

[8] S. von Goeler et al., Phys. Rev. Lett. **33** (1974) 1201.

[9] R. J. Hastie, Astrophysics and Space Science **256** (1998) 177.

[10] A. Jacchia et al., Phys. Fluids **B 3** (1991) 3033.

[11] B. Coppi et al., Nucl. Fusion **21** (1981) 1363.

[12] B. Coppi et al., Phys. Rev. Lett. **41** (1978) 551.

[13] K. W. Gentle et al., Plasma Phys. Controlled Fusion **26** (1984) 1407.

[14] A. A. Bagdasarov et al., in *Plasma Physics and Controlled Fusion Research (Proc.* 10^{th} *Int.*

Conf., London, 1984), Vol. 1 IAEA, Vienna, pages 181–192, 1985.

[15] K. W. Gentle et al., Plasma Physics and Controlled Fusion **29** (1987) 1077.

[16] U. Stroth et al., Phys. Rev. Lett. **82** (1999) 928.

[17] J. Koponen et al., Nucl. Fusion **40** (2000) 365.

[18] K. Tanaka et al., Nuclear Fusion **46** (2006) 110, Corrigendum in Plasma Phys. Controlled Fusion **48** (2008) 039801.

[19] P. C. Efthimion et al., Physics of Fluids B: Plasma Physics **3** (1991) 2315.

[20] K. Gentle et al., Nuclear Fusion **32** (1992) 217.

[21] K. Nagashima et al., Nucl. Fusion **33** (1993) 1677.

[22] D. Baker et al., Nucl. Fusion **38** (1998) 485.

[23] H. Takenaga et al., Nuclear Fusion **39** (1999) 1917.

[24] D. Baker et al., Nucl. Fusion **40** (2000) 799.

[25] X. Gao et al., Nucl. Fusion **48** (2008) 035009.

[26] A. G. Peeters et al., in *Europhysics Conference Abstracts (Proc. of the 24th EPS Conference on Controlled Fusion and Plasma Physics, Berchtesgaden, 1997)*, edited by M. Schittenhelm et al., volume 21A, part IV, pages 1469–1472, Petit-Lancy, 1997, EPS.

[27] K. Krieger et al., Nucl. Fusion **30** (1990) 2392.

[28] C. Angioni et al., Nuclear Fusion **44** (2004) 827.

[29] D. R. Baker et al., Physics of Plasmas **8** (2001) 4128.

[30] R. Dux et al., Plasma Physics and Controlled Fusion **45** (2003) 1815.

[31] M. R. Wade et al., Physics of Plasmas **2** (1995) 2357.

[32] R. Dux et al., Nuclear Fusion **39** (1999) 1509.

[33] T. Parisot et al., Plasma Physics and Controlled Fusion **50** (2008) 055010.

[34] L. R. Baylor et al., Nucl. Fusion **31** (1991) 1249.

[35] P. C. Efthimion et al., Phys. Rev. Lett. **75** (1995) 85.

[36] JET Team (prepared by K.-D. Zastrow), Nuclear Fusion **39** (1999) 1891.

[37] K.-D. Zastrow et al., Plasma Physics and Controlled Fusion **46** (2004) B255.

[38] D. Stork et al., Nuclear Fusion **45** (2005) S181.

[39] E. J. Synakowski et al., Phys. Rev. Lett. **65** (1990) 2255.

[40] E. J. Synakowski et al., Physics of Fluids B: Plasma Physics **5** (1993) 2215.

[41] E. J. Synakowski et al., Phys. Rev. Lett. **75** (1995) 3689.

[42] H.-S. Bosch et al., Plasma Physics and Controlled Fusion **39** (1997) 1771.

[43] M. R. Wade et al., Phys. Rev. Lett. **84** (2000) 282.

[44] R. Dux et al., Journal of Nuclear Materials **313–316** (2003) 1150.

[45] M. E. Puiatti et al., Physics of Plasmas **13** (2006) 042501.

[46] C. Giroud et al., Nuclear Fusion **47** (2007) 313.

[47] R. Guirlet et al., Nuclear Fusion **49** (2009) 055007.

[48] M. Yoshinuma et al., Nuclear Fusion **49** (2009) 062002.

[49] R. Guirlet et al., Plasma Phys. Controlled Fusion **48** (2006) B63.

[50] S. Ejima et al., Phys. Rev. Lett. **32** (1974) 872.

[51] J. D. Callen et al., Phys. Rev. Lett. **38** (1977) 491.

[52] G. L. Jahns et al., Nucl. Fusion **18** (1978) 609.

[53] E. D. Fredrickson et al., Phys. Rev. Lett. **65** (1990) 2869.

[54] F. D. Luca et al., Nuclear Fusion **36** (1996) 909.

[55] F. Ryter et al., in *Europhysics Conference Abstracts (CD-ROM), Proc. of the 26th EPS Conference on Controlled Fusion and Plasma Physics, Maastricht, 1999*, edited by C. Bastian et al., volume 23J, pages 1433–1436, Geneva, 1999, EPS.

[56] B. Lloyd, Plasma Physics and Controlled Fusion **40** (1998) A119.

[57] R. Prater, Phys. Plasmas **11** (2004) 2349.

[58] F. Imbeaux et al., Plasma Physics and Controlled Fusion **43** (2001) 1503.

[59] F. Ryter et al., Nuclear Fusion **43** (2003) 1396.

[60] F. Ryter et al., Physical Review Letters **95** (2005) 085001.

[61] J. C. DeBoo et al., Nuclear Fusion **45** (2005) 494.

[62] P. Mantica et al., Fusion Science and Technology **53** (2008) 1152.

[63] A. Jacchia et al., Nucl. Fusion **42** (2002) 1116 .

[64] X. Garbet et al., Plasma Physics and Controlled Fusion **46** (2004) 1351, Addendum in Plasma Physics and Controlled Fusion **47**, 6, pp. 957–958 (2005).

[65] F. Ryter et al., Plasma Physics and Controlled Fusion **48** (2006) B453.

[66] U. Stroth, Plasma Phys. Controlled Fusion **40** (1998) 9.

[67] S. Inagaki et al., Nucl. Fusion **46** (2006) 133.

[68] L. Giannone et al., Nucl. Fusion **32** (1992) 1985.

[69] H. J. Hartfuß et al., Plasma Phys. Controlled Fusion **36** (1994) B17.

[70] S. Eguilior et al., Plasma Physics and Controlled Fusion **45** (2003) 105.

[71] M. Hirsch et al., Plasma Physics and Controlled Fusion **50** (2008) 053001.

[72] X. Litaudon, Plasma Physics and Controlled Fusion **48** (2006) A1.

[73] A. Fujisawa, Plasma Physics and Controlled Fusion **45** (2003) R1.

[74] P. Mantica et al., Plasma Physics and Controlled Fusion **44** (2002) 2185.

[75] T. Shimozuma et al., Nuclear Fusion **45** (2005) 1396.

[76] P. Mantica et al., Physical Review Letters **96** (2006) 095002.

[77] A. Marinoni et al., Plasma Physics and Controlled Fusion **48** (2006) 1469.

[78] A. Casati et al., Phys. Plasmas **14** (2007) 092303.

[79] T. Estrada et al., Nuclear Fusion **47** (2007) 305.

[80] U. Stroth et al., Phys. Rev. Lett. **86** (2001) 5910.

[81] E. D. Fredrickson et al., Physics of Plasmas **7** (2000) 5051.

[82] D. V. Eester et al., Plasma Phys. Controlled Fusion **51** (2009) 044007.

[83] F. Ryter et al., in *Proc. of the 22nd IAEA Conference Fusion Energy (CD-Rom), Geneva, Switzerland, Ocotber 2008*, volume IAEA-CSP-25/CD, pages IAEA–CN–165/EX/P5–19, Vienna, 2008, IAEA.

[84] P. Mantica et al., Phys. Rev. Lett. **102** (2009) 175002.

[85] T. C. Luce et al., Phys. Rev. Lett. **68** (1992) 52.

[86] C. Petty et al., Nucl. Fusion **34** (1994) 121 .

[87] G. Hogeweij et al., Phys. Rev. Lett. **76** (1996) 632.

[88] P. Mantica et al., Phys. Rev. Lett. **85** (2000) 4534.

[89] P. Mantica et al., Phys. Rev. Lett. **95** (2005) 185002.

[90] K. W. Gentle et al., Phys. Plasmas **13** (2006) 012311.

[91] T. C. Luce et al., in *Europhysics Conference Abstracts (CD-ROM, Proc. of the 32nd EPS Conference on Plasma Physics, Tarragona, 2005)*, edited by C. Hidalgo et al., volume 29C, pages P–5.308, Geneva, 2005, EPS.

[92] P. Mantica et al., Plasma Physics and Controlled Fusion **48** (2006) 385.

[93] X. Garbet et al., Physics of Plasmas **12** (2005) 082511.

[94] J. Weiland et al., Physics of Fluids B: Plasma Physics **5** (1993) 1669.

[95] H. Nordman et al., Plasma Physics and Controlled Fusion **43** (2001) 1765.

[96] M. G. Haines, Plasma Physics and Controlled Fusion **38** (1996) 897.

[97] J. S. deGrassie, Plasma Phys. Controlled Fusion **51** (2009) 124047.

[98] P. Diamond et al., Nucl. Fusion **49** (2009) 045002.

[99] K. H. Burrell et al., Nucl. Fusion **28** (1988) 3.

[100] H. Weisen et al., Nucl. Fusion **29** (1989) 2187.

[101] S. D. Scott et al., Phys. Rev. Lett. **64** (1990) 531.

[102] A. Kallenbach et al., Plasma Phys. Controlled Fusion **33** (1991) 595.

[103] D. Nishijima et al., Plasma Physics and Controlled Fusion **47** (2005) 89.

[104] P. C. de Vries et al., Plasma Phys. Controlled Fusion **48** (2006) 1693.

[105] S. Kaye et al., Nucl. Fusion **49** (2009) 045010.

[106] A. G. Peeters et al., Physics of Plasmas **12** (2005) 072515.

[107] A. G. Peeters et al., Physical Review Letters **98** (2007) 265003.

[108] T. S. Hahm et al., Phys. Plasmas **14** (2007) 072302.

[109] K. Nagashima et al., Nucl. Fusion **34** (1994) 449.

[110] K. Ida et al., Phys. Rev. Lett. **74** (1995) 1990.

[111] K. Ida et al., J. Phys. Soc. Jpn **67** (1998) 4089.

[112] A. Manini et al., Nuclear Fusion **43** (2003) 490.

[113] Y. Sakamoto et al., Plasma Physics and Controlled Fusion **48** (2006) A63.

[114] M. Yoshida et al., Phys. Rev. Lett. **103** (2009) 065003.

[115] W. M. Solomon et al., Phys. Plasmas **17** (2010) 056108.

[116] M. Yoshida et al., Nucl. Fusion **47** (2007) 856.

[117] M. Yoshida et al., Nucl. Fusion **49** (2009) 115028.

[118] W. M. Solomon et al., Phys. Rev. Lett. **101** (2008) 065004.

[119] W. Solomon et al., Nucl. Fusion **49** (2009) 085005.

[120] K.-D. Zastrow et al., Nucl. Fusion **38** (1998) 257.

[121] T. Tala et al., Plasma Phys. Controlled Fusion **49** (2007) B291.

[122] T. Tala et al., Physical Review Letters **102** (2009) 075001.

[123] G. Tardini et al., Nucl. Fusion **49** (2009) 085010.

[124] P. Mantica et al., Physics of Plasmas **17** (2010) 092505.

[125] W. D. Lee et al., Phys. Rev. Lett. **91** (2003) 205003.

[126] J. Rice et al., Nucl. Fusion **44** (2004) 379.

[127] G. M. D. Hogeweij et al., Plasma Physics and Controlled Fusion **34** (1992) 641.

[128] N. Deliyanakis et al., Plasma Physics and Controlled Fusion **36** (1994) 1391.

[129] J. C. DeBoo et al., Nucl. Fusion **39** (1999) 1935.

[130] F. Imbeaux et al., Phys. Rev. Lett. **96** (2006) 045004.

[131] U. Stroth et al., Plasma Phys. Controlled Fusion **38** (1996) 611, Corrigendum in Plasma Phys. Contr. Fus., **38** 1087 (1996).

[132] V. F. Andreev et al., Plasma Phys. Controlled Fusion **46** (2004) 319.

[133] J. D. Callen et al., Plasma Phys. Controlled Fusion **39** (1997) B173.

[134] H. Walter et al., Plasma Phys. Controlled Fusion **40** (1998) 1661.

[135] B. van Milligen et al., Nuclear Fusion **42** (2002) 787.

[136] S. Inagaki et al., Plasma Phys. Controlled Fusion **46** (2004) A71.

[137] S. Inagaki et al., Plasma Physics and Controlled Fusion **48** (2006) A251.

[138] N. Tamura et al., Nuclear Fusion **47** (2007) 449.

[139] P. Galli et al., Nucl. Fusion **39** (1999) 1355.

[140] G. M. D. Hogeweij et al., Plasma Phys. Controlled Fusion **42** (2000) 1137.

[141] F. Ryter et al., Nuclear Fusion **40** (2000) 1917.

[142] X. L. Zou et al., Plasma Phys. Controlled Fusion **42** (2000) 1067.

[143] J. E. Kinsey et al., Phys. Plasmas **5** (1998) 3974.

[144] J. P. Christiansen, Plasma Physics and Controlled Fusion **49** (2007) 1309.

[145] D. del Castillo-Negrete et al., Nuclear Fusion **48** (2008) 075009.

[146] V. Naulin et al., J. Plasma Fusion Res. SERIES **8** (2009) 55.

[147] Y. Peysson, Plasma Physics and Controlled Fusion **35** (1993) B253.

[148] C. Petty et al., Nuclear Fusion **39** (1999) 1421.

[149] M. Zerbini et al., Plasma Physics and Controlled Fusion **41** (1999) 931.

[150] Y. Torii et al., Plasma Physics and Controlled Fusion **43** (2001) 1191.

[151] K. Saito et al., Plasma Physics and Controlled Fusion **44** (2002) 103.

[152] F. Leuterer et al., Nuclear Fusion **43** (2003) 744.

[153] H. Laqua et al., Nuclear Fusion **43** (2003) 1324.

[154] K. K. Kirov et al., Plasma Physics and Controlled Fusion **44** (2002) 2583.

[155] D. V. Eester, Plasma Physics and Controlled Fusion **46** (2004) 1675.

[156] K. K. Kirov et al., Plasma Physics and Controlled Fusion **48** (2006) 245.

[157] E. A. Lerche et al., Plasma Physics and Controlled Fusion **50** (2008) 035003.

[158] S. Inagaki et al., Phys. Rev. Lett. **92** (2004) 055002.

[159] M. Yakovlev et al., Physics of Plasmas **12** (2005) 092506.

[160] G. Spakman et al., Nucl. Fusion **48** (2008) 115005.

[161] J. G. Cordey et al., Plasma Phys. Controlled Fusion **36** (1994) A267.

[162] S. V. Neudatchin et al., Plasma Phys. Controlled Fusion **43** (2001) 661.

[163] S. V. Neudatchin et al., Plasma Physics and Controlled Fusion **44** (2002) A383.

[164] L. Frassinetti et al., Nuclear Fusion **47** (2007) 135.

[165] F. Turco et al., Physics of Plasmas **16** (2009) 062301.